SMALL ANGLE X-RAY SCATTERING
OF THE THYLAKOID MEMBRANES
OF *RHODOPSEUDOMONAS SPHEROIDES*
IN AQUEOUS SUSPENSIONS

E. H. PAPE, W. MENKE, D. WEICK, *and* R. HOSEMANN

From the Max Planck Institut für Züchtungsforschung (Erwin Baur Institut), Köln-Vogelsang, West Germany, and the Fritz Haber Institut der Max Planck Gesellschaft, Dahlem, Berlin, Germany. Dr. Pape's present address is Institut für Biophysik und Strahlenbiologie, University of Freiburg, West Germany.

ABSTRACT   The diffraction patterns of particles which have the shape of hollow spheres, i.e. vesicles, can be satisfactorily analyzed by means of a new formula of Weick (1974). This formula is used for the small angle X-ray scattering analysis of aqueous suspensions of thylakoids of *Rhodopseudomonas spheroides*. Some essential results are: (*a*) The membrane has a rather asymmetric structure with one layer of low electron density at its inner side and two layers of high electron density near the outer surface of the thylakoids. (*b*) The distance of the electron density maxima of the latter two layers is 45 ± 5 Å. (*c*) Between the two maxima is a region of an electron density nearly equal to that of water. (*d*) The sequence of the peaks is $- + 0 +$ with increasing radius. The peaks extend over an interval of 120 ± 10 Å. (*e*) The thylakoids are strikingly of the same size. Their diameters, if defined by the outmost layer, vary statistically by about 4% and have an average value of approximately 640 Å.

INTRODUCTION

It is of great importance for an understanding of the primary reactions of photosynthesis to learn more about the molecular structure of the respective membrane systems. In this paper thylakoid membranes of the phototropic bacterium *Rhodopseudomonas spheroides* are investigated by means of small angle X-ray scattering. In aqueous suspensions these thylakoids have the shape of spherical vesicles with mostly a constant diameter (Fig. 1). After Schmitz (1967) these thylakoids contain 53% proteins and 37% lipids. Obviously the primary processes of photosynthesis take place inside the thylakoid membranes. It is therefore of great interest to know more about their molecular structure, which can be deciphered by small angle X-ray scattering, if the sample is suitably prepared and the structure not too much distorted.
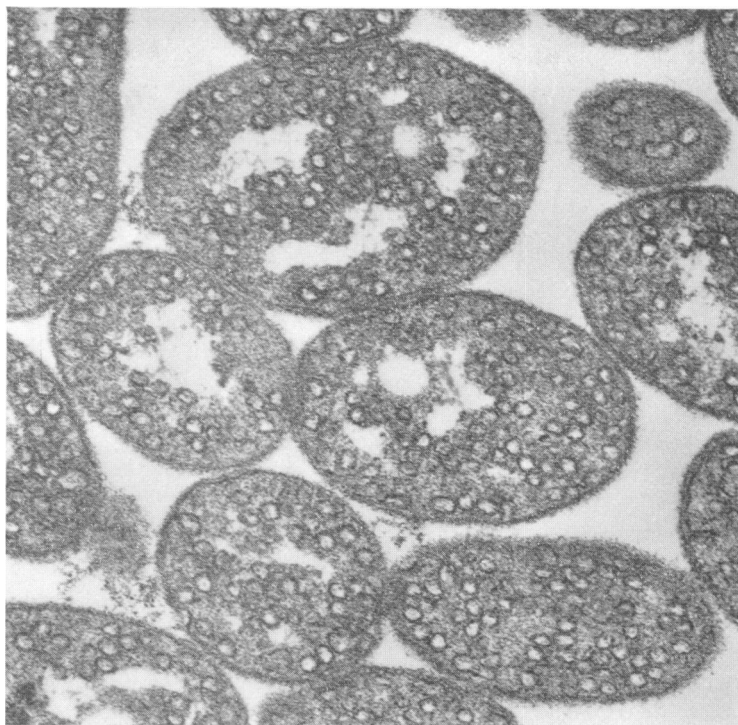
FIGURE 1   Electronmicrograph of *Rhodopseudomonas spheroides* ($\times 40,000$).

PREPARATION OF THE SAMPLE

The cultivation of *Rh. spheroides* is described in the papers of Schmitz (1967) and Wiessner (1960) as well as the isolation of the thylakoids by disruption of the cells and subsequent fractioning centrifugation.

The isolated thylakoids were filled as aqueous suspensions into Mark capillars.[1] The X-ray small angle scattering of these suspensions was investigated in a Kratky small angle diffraction chamber[1] with CuKα radiation monochromatizated with a quartz crystal of the Johansson type.[2]

The slit smearing was eliminated according to the Lake procedure (1967) with the computer of the University of Köln.

The small angle X-ray scattering was photographically registered on Doneo Adox Clear Base films and analyzed in a microphotodensitometer of Joyce-Loebl.[3] The exposure time was in the order of 300 h. The background scattering was eliminated by subtracting the intensity curves of capillars filled with pure water. A typical scattering diagram of *Rh. spheroides* thylakoids is given in Fig. 2. The diagram is
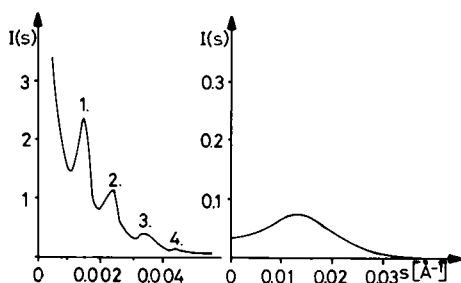

FIGURE 2 Small angle scattering (relative units) corrected from slit smearing of isolated thylakoids of *Rhodopseudomonas spheroides*. Exposed 300 h with CuKα crystalmonochromatizated in a Kratky chamber.

corrected for the slit smearing and background scattering. The central diffraction extends over $2\vartheta \leq 10$ mrad as a continuous small angle scattering, modulated by four peaks with a distance of ca. 3 mrad. In the right-hand figure the outer region of the small angle X-ray scattering is enlarged 10-fold and shows an additional diffuse maximum at ~ 28 mrad. This gives information on the inner structure of the membrane while the modulations of the central peak obviously are subsidiary interferences due to the shape of the vesicles.

THE BACKGROUND OF ANALYSIS OF THE SMALL ANGLE SCATTERING WITH CONVOLUTION OPERATIONS

For the first time, Langridge, Barron, and Sistrom (1964) have studied the small angle scattering of *Rh. spheroides* thylakoids and have found subsidiary maxima corresponding to the maxima 2, 3, 4 of Fig. 2 and a diffuse outer interference corresponding to the right-hand part of Fig. 2. Because of an inferior resolving power they could not find the first peak 1 of Fig. 2. Within the experimental error the other maxima, which they found to have Bragg-distances of 240, 170, and 131 Å agree with our values of 247, 175, and 133 Å. The peak 1 corresponds to 400 Å. In order to analyze the diffraction pattern we assume that the electron density distribution depends practically only on the distance r of the center of the vesicles and has no azimuthal variation. This assumption is based on electronmicroscopical observations by Giesbrecht, finding lattice-like surface structures only in *Rh. viridis* (Giesbrecht and Drews, 1966) but not in *Rh. spheroides* (Giesbrecht, 1969).

Obviously in the thylakoids of *Rh. spheroides* the structure along the surface is so irregular, that interference phenomena in the azimuthal directions can be practically disregarded (Menke and Weichmann, 1968). If the electron density distribution $\rho(\vec{x})$ of a vesicle with the center at $x = 0$ only depends on $|\vec{x}| = r$, its scattering amplitude $F(s)$ is given by the well-known formula

$$F(s) = (2/s) \int_0^\infty r\rho(r) \sin (2\pi sr) \, dr, \qquad (1)$$

with

$$s = (2 \sin d\theta)/\lambda. \tag{2}$$

Following Weick (1974), we introduce the auxiliary functions

$$g(x) = \begin{cases} r\rho(r) & \text{for } x = r \geq 0 \\ 0 & \text{for } x < 0 \end{cases} \tag{3}$$

and

$$P(r) = 2 \int_0^\infty s^2 F^2(s) \cos (2\pi sr) \, ds, \tag{4}$$

which are related by the following equation:

$$P(r) = 2\tilde{g}^2(r) - \widehat{gg}(r). \tag{5}$$

$\tilde{g}^2$ and $\widehat{gg}$ denote the convolution square and convolution product of the function $g(x)$, as defined by Hosemann and Bagchi (1962):

$$\tilde{g}^2(r) = \int_{-\infty}^{+\infty} g(x)g(x - r) \, dx \tag{6}$$

$$\widehat{gg}(r) = \int_{-\infty}^{+\infty} g(x)g(r - x) \, dx. \tag{7}$$

Since the function $P(r)$ can be calculated from the scattering intensity

$$I(s) \sim F^2(s) \tag{8}$$

directly (except for a scaling factor) it may be considered as an "observed" quantity, from which we may try to determine $g(x)$ with the help of Eq. 5. If this can be managed, the radial density distribution $\rho(r)$ is also known according to Eq. 3.

The solution of this problem is facilitated by the fact that, as we shall see below, the two contributions on the right-hand side of Eq. 5, $2\tilde{g}^2$ and $-\widehat{gg}$, do not overlap. We then have in $P(r)$ two independent statements about the structure.

However, it is to be expected, that the vesicle diameters deviate from their mean value $\bar{D}$ with some frequency distribution $H(x)$ ($x = D - \bar{D}$). Therefore only the average intensity can be observed, and hence we obtain from Eq. 4 an average of the function $P(r)$:

$$\bar{P}(r) = 2 \tilde{g}^2 - \widehat{\widehat{gg}H}. \tag{9}$$

THE EVALUATION OF SMALL ANGLE SCATTERING

Fig. 3 shows the observed function $I(s)$ multiplied with s^2 and Fig. 4 shows its Fourier transform P for positive arguments $x = r$. In accordance with the theoretical expectation for spherical shell structures (see Weick, 1974), this function has values different from zero in two separate domains, an interior domain (A)
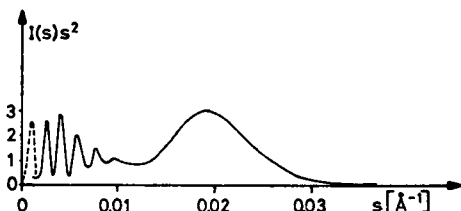
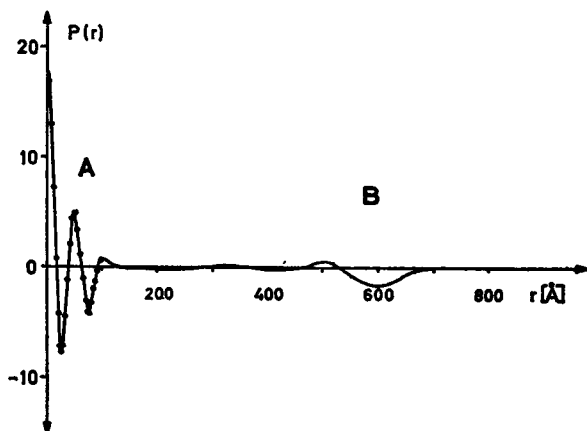FIGURE 3   Small angle scattering of Fig. 2 multiplied s^2.

FIGURE 4   The function $P(r)$, —— calculated from the observed intensity with the help of Eq. 4, ● ● ● drawn from the calculated $\bar{g}^2_{\text{III}}$ of Table I with the parameters of Table IV.

$$r \leq 120 \text{ Å}, \tag{10}$$

and an exterior domain (B)

$$450 \text{ Å} \leq r \leq 700 \text{ Å}. \tag{11}$$

We may then write

$$P(r) = P_A(r) + P_B(r). \tag{12}$$

(P_A and P_B are zero outside the domains A and B, respectively) and shall identify P_A with the first term of Eq. 9, P_B with the second one:

$$2\bar{g}^2(r) = P_A(r) \tag{13}$$

$$-\widehat{\bar{g}\bar{g}H}(r) = P_B(r). \tag{14}$$

The further analysis starts with Eq. 13, which has several solutions $g(x)$. These are determined (except for a possible translation and a change of sign) in the next

section. Thereupon Eq. 14 will enable us to discriminate between the different solutions of Eq. 13 and to determine the mean diameter of the vesicles.

The Convolution Roots of $P_A(r)$

Although in general there exist infinitely many functions having the same convolution square, in practical cases the number of significant solutions may be considerably restricted, if arguments of symmetry, simplicity, or physical plausibility are taken into account (see Hosemann and Bagchi, 1962). The following discussion provides another example of such methods, which may be inconclusive in a rigorous mathematical sense, but seems to be justified in view of the limited accuracy of the experimental data analyzed in this way.

In Table I $P_A(r)/2$, as determined from the observed intensity, is listed (column 2). Column 3 contains an approximate analytical representation of this function,

$$G(r) \approx \tfrac{1}{2} P_A(r),\tag{15}$$

consisting of Gaussians of equal widths in symmetrical and equidistant arrangement:

$$G(x) = \sum_{\nu=-4}^{4} G_\nu \exp\left[-(x - \nu d)^2/a^2\right].\tag{16}$$

The parameters G_ν, d, and a are listed in Table II. We shall now try to find the solutions of the equation

$$g^2(x) = G(x).\tag{17}$$

Under the plausible restriction, that the solutions are also composed of Gaussians, $g(x)$ will be of the form

$$g(x) = (2/a\sqrt{\pi})^{1/2} \sum_{n=1}^{5} g_n \exp\left[-2(x - r_n)^2/a^2\right],\tag{18}$$

with

$$r_n = r_o + n d.\tag{19}$$

(The normalizing factor has been taken out of the sum for convenience). The parameter r_o determines the diameter of the vesicle and is so far entirely unspecified. It may even differ for the various vesicles without affecting the convolution square. The weight factors g_n must obey a set of algebraic equations, which is obtained by equating the convolution square of g,

$$g^2(x) = \sum_n \sum_m g_n g_m \exp\left\{-[x - (r_n - r_m)]^2/a^2\right\},\tag{20}$$

TABLE I
EXPERIMENTAL DATA

r	$\frac{1}{2}P_A(r)$	$G(r)$	$\tilde{g}^2_{III}$
$\mathring{A}$			
0	95.0	94.9	95.7
2	92.3	92.4	93.7
4	86.9	85.0	87.9
6	79.5	73.7	78.7
8	69.0	59.5	66.7
10	53.1	43.7	52.7
12	37.1	27.6	37.5
14	22.4	12.1	22.0
16	8.6	−1.8	7.2
18	−5.1	−13.6	−6.2
20	−17.4	−22.9	−17.5
22	−29.9	−29.5	−26.2
24	−33.4	−33.3	−31.8
26	−34.1	−34.2	−34.4
28	−33.2	−32.6	−34.0
30	−30.6	−28.7	−30.8
32	−25.7	−23.0	−25.3
34	−17.4	−16.0	−18.1
36	−9.1	−8.1	−9.7
38	−1.0	−0.1	−9.8
40	7.2	7.9	7.6
42	15.4	15.1	15.3
44	21.7	21.4	21.8
46	27.3	26.2	26.7
48	29.4	29.4	29.6
50	30.7	30.7	30.7
52	30.0	30.0	29.8
54	27.1	27.6	27.2
56	22.8	23.7	23.3
58	17.3	18.8	18.2
60	12.9	13.2	12.5
62	6.9	7.5	6.6
64	1.7	1.8	0.9
66	−4.1	−3.4	−4.3
68	−8.7	−7.9	−8.7
70	−12.0	−11.5	−12.2
72	−15.0	−14.1	−14.5
74	−15.9	−15.6	−15.8
76	−15.8	−16.0	−16.0
78	−15.1	−15.4	−15.3
80	−14.1	−13.9	−13.8
82	−12.0	−11.9	−11.8
84	−9.8	−9.5	−9.4
86	−7.2	−6.9	−6.9
88	−5.0	−4.4	−4.4
90	−2.2	−2.2	−2.2
92	−0.1	−0.2	−0.3
94	1.6	1.3	1.2
96	2.6	2.5	2.2
98	3.3	3.3	2.8
100	3.7	3.7	3.0
102	3.3	3.8	2.9
104	2.8	3.6	2.6
106	1.6	3.3	2.2
108	0.9	2.8	1.8

with the right-hand side of Eq. 16:

$$\sum_{n=1}^{5-\nu} g_n g_{n+\nu} = G_\nu, \qquad (\nu = 0, 1, \cdots 4). \quad (21)$$

Taking the G_ν from Table II, we find by a seminumerical procedure (carried out on the Hewlett-Packard [Palo Alto, Calif.] table computer), that there exist (except for a factor ± 1) four different real solutions of this system, which are listed in Table III. The sign was chosen in such a way, that

$$\sum_{n=1}^{5} g_n > 0. \qquad (22)$$

Solutions I$'$ and II$'$ are the mirror images of solutions I and II, respectively. The corresponding functions $g(x)$ are shown in Fig. 5. The parameter r_0 is put equal to 195 Å, a result following from the discussion of the subsequent section.

Calculation of the Convolution Products and Comparison with $P_B(r)$

The convolution product of $g(x)$ is given by the following equation:

$$\widehat{gg}(x) = \sum_n \sum_m g_n g_m \exp \{ -[x - (r_n + r_m)]^2/a^2 \}. \qquad (23)$$

This expression differs from that for $g^2(x)$ (Eq. 20) only in a sign in the exponent: the quantity $(r_n - r_m)$, which represents the position of the maximum of one term of $g^2(x)$, is now replaced by

$$r_n + r_m = 2r_0 + (n + m) d. \qquad (24)$$

TABLE II

PARAMETERS G_ν, d, AND a

ν.....	0	1	2	3	4
G_ν....	96.8	−37.3	32.0	−16.8	4.1

$G_{-\nu} = G_\nu$, $a = 13$ Å, $d = 25$ Å.

TABLE III

REAL SOLUTIONS

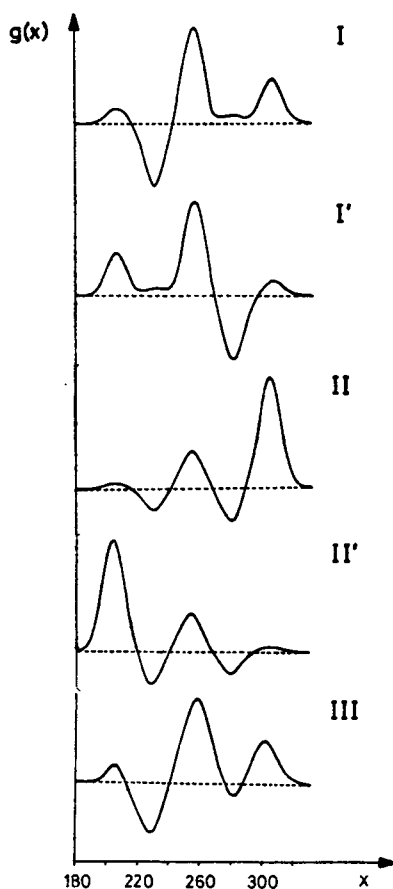|	g_1	g_2	g_3	g_4	g_5
I	1.18	−5.06	7.53	0.64	3.47
I$'$	3.47	0.64	7.53	−5.06	1.18
II	0.46	−1.76	2.94	−2.66	8.82
II$'$	8.82	−2.66	2.94	−1.76	0.46

FIGURE 5 The different functions $g(x)$ obtained as convolution roots from the central part of Fig. 4 and with the parameters of Tables II–IV.

Therefore, the domain covered by the function $\widehat{gg}(x)$, lies beyond the point $x = 2r_o$. Besides this, owing to the asymmetry of the different solutions $g(x)$, the convolution product has no center of symmetry.

Supposing all vesicles had exactly the same diameter, $-\widehat{gg}(r)$ should equal $P_B(r)$ and Eq. 14 would be the most suitable starting point for the determination of the structure. However, Fig. 4 indicates, that in our case the vesicles have a certain range of diameters. For convenience, we shall assume a centrosymmetric distribution function of the Gaussian type:

$$H(x) = \left(1/\sqrt{\pi}b\right) \exp\left(-x^2/b^2\right). \tag{25}$$

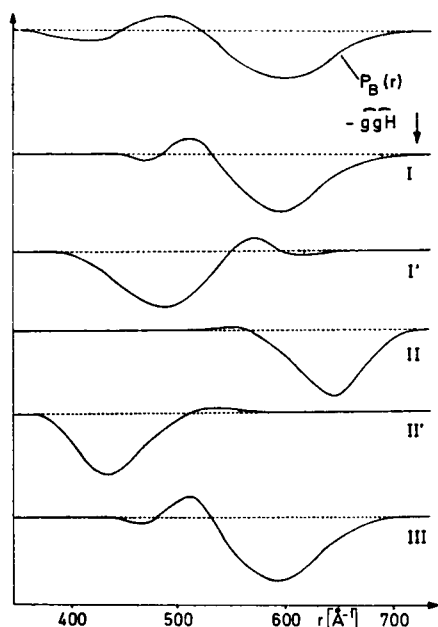Fig. 6 shows the observed funtion $P_B(r)$ and the calculated functions $-\widehat{ggH}(r)$ for

FIGURE 6 —— The convolution products of the $g(x)$ functions of Fig. 5 folded with the function $H(x)$ of Eq. 25 and compared with the observed function $P_B(r)$.

the four solutions. The parameters r_o and b were so chosen as to give the best possible agreement between the observed curve and that calculated from solution I.

Taking into consideration that: (a) there are certainly experimental errors, (b) the structures $g(x)$ are obtained by an idealization of the observed $P_A(r)$ (approximation by a seven-parameter function), and (c) the frequency distribution of vesicle diameters need not be centrosymmetric, as assumed here for simplicity, we cannot expect to find a perfect agreement in the domain B. However there is a distinct similarity in case of solution I, whereas the remaining solutions (I', II, II') show a quite dissimilar qualitative behavior. Therefore these latter solutions may be discarded with high probability.

A refinement of solution I can be obtained by admitting small deviations from the equidistant arrangement and varying widths of the single Gaussians in Eq. 18. With the help of a program by D. W. Marquardt (Least Squares Estimation of Nonlinear Parameters, DuPont de Nemours & Co., Wilmington, Del.) a best fit of $P_A(r)$ was obtained with the parameters listed in Table IV.

The function $g(x)$ obtained in this way is shown in Fig. 5 III. Its qualitative behavior is similar to that of solution I. Its convolution square equals the experimentally determined $P_A(r)/2$ considerably better than the seven-parameter function 15 (see Table I, column 4), while the function $-\widehat{gg}H$ is nearly the same as for solution I. The distance of the two positive peaks is somewhat smaller than in solution

TABLE IV

PARAMETERS YIELDING A BEST-FIT CURVE
FOR $P_A(r)$

n.....	1	2	3	4	5
a_n	6.6	12.1	13.5	17.4	12.7
r_n	228.3	238.3	270.0	298.1	322.2
g_n	1.45	−4.13	6.86	−2.33	5.04

I ($\sim$45 Å instead of 50 Å), a fact which indicates that the precision of such statements should not be estimated too high.

THE SIGN OF $g(x)$

The only remaining ambiguity is the sign of $g(x)$. We have—so far arbitrarily—defined it by the condition 22, which needs to be justified. This may be done by considering the average mass-density of the thylakoids, which must be higher than that of water. This follows from the fact that a sedimentation is achieved in a high-speed centrifuge. The density difference may be estimated from the time of sedimentation to be of the order of 0.1 g/cm³. This is in good agreement with the results for the thylakoid membrane of chloroplasts, which contain nearly the same amounts of proteins and lipids as the thylakoids of *Rhodopseudomonas spheroides*. The average density of the chloroplasts has recently been determined with high precision by Menke and co-workers (to be published) to be 1.136 g/cm³.

Since for all lighter elements except hydrogen the ratio of electronic number and mass is very nearly the same and it may be assumed that the mass contribution of hydrogen in the thylakoid membrane is not very different from that in water, we may conclude that also the average electron density should exceed that of water by about 10%. Taking into account that the small angle scattering is sensitive only to the electron density difference between the structure and the surrounding medium, we must require that the volume integral of $\rho(r)$, as obtained from $g(r)$ (Eq. 3) be positive:

$$4\pi \int_0^\infty \rho(r)r^2\, dr = 4\pi \int_0^\infty rg(r)\, dr > 0. \qquad (26)$$

It is easily verified that this condition would be violated, if we had chosen the opposite sign for $g(x)$.

Our final result shown in Fig. 5 III makes it probable that the uttermost positive layer mainly consists of proteins, whereas the inner negative layer at 230 Å should be preponderantly composed of lipids. Indeed, Reuss (1972) was able to demonstrate the presence of proteins on the outer surface of thylakoids by means of serological investigations. Consistent with the distance of 45 Å of the two positive peaks in Fig. 5 III, electronmicrographs of negatively contrasted thylakoids gave

evidence of 40–50 Å thick membranes with an intermediate looser packed zone in which the contrasting agent is incorporated (Menke and Weichan, 1968). This zone might correspond to the negative peak at 280 Å in Fig. 5 III. In the electron-micrograph, beside the two layers with higher density the small inner layer at 200 Å with lower positive density would not yet be observed. According to Menke and Weichan (1968) it appears that in the course of preparation of the electron-microscopic specimens the lipids come out of the thylakoid membrane and are distributed on the supporting foil. Therefore, in general, lipids cannot be made visible inside the membrane by electronmicroscopy and, hence, the thickness of the membrane appears to be only 40–50 Å.

All these observations let us conclude that the molecular structure of the thylakoid membrane of *Rh. spheroides* is related to a structure, which Hosemann and Kreutz (1966, 1970) have calculated for the thylakoid membrane of chloroplasts, although remarkable differences exist with respect to their thickness. Last but not least it may be noted that according to recent serological investigations the two-layer model may be only regarded as a first rough approximation for the structure of thylakoid membranes.

REFERENCES

GIESBRECHT, P. 1969. Die wichtigsten Feinstrukturen der Bakterien im elektronenmikroskopischen Bild. *In* Bildatlas Pathogener Mikroorganismen. Henneberg, editor. Gustav Fischer Verlag, Stuttgart, West Germany.

GIESBRECHT, P., and G. DREWS. 1966. *Arch. Mikrobiol.* **54**:297.

HOSEMANN, R., and S. N. BAGCHI. 1962. Direct Analysis of Diffraction by Matter. North-Holland Publishing Co., Amsterdam.

HOSEMANN, R., and W. KREUTZ. 1966. *Naturwissenschaften.* **12**:53, 298.

KREUTZ, W. 1970. *Adv. Bot. Res.* **3**:54.

LAKE, J. A. 1967. *Acta Crystallogr.* **23**:191.

LANGRIDGE, R., P. D. BARRON, and W. R. SISTROM. 1964. *Nature (Lond.).* **204**:97.

MENKE, W., and C. WEICHAN. 1968. *Arch. Mikrobiol.* **60**:1.

REUS, W. 1972. *Arch. Mikrobiol.* **82**:265.

SCHMITZ, R. 1967. *Z. Naturforsch.* **22**:645.

WEICK, D. 1974. *Biophys. J.* **14**:233.

WIESSNER, W. 1960. *Flora (Jena).* **149**:1.